charge on the complex constant. In the first reduction step the protonation occurs on the ligand, and in the second step it takes place on the metal.

Acknowledgment. We are indebted to the Natural Sciences and Engineering Research Council of Canada for financial support of this research and to K. Moffat and V. Stratton for performing some of the initial experiments in this area.

Registry No. $K_4[Fe(CN)_5(NO_2)]$, 14709-58-1; $K_4[Fe(CN)_5(4\text{-NIM})]$, 95531-72-9; $Na_5[Fe(CN)_5(SO_3)]$, 12169-60-7; $[Fe(CN)_5(4\text{-NIM})]^{4-}$, 95531-73-0; $[Fe(CN)_4(4\text{-NIMH})]^{3-}$, 95531-74-1; $[Fe(CN)_5NO]^{2-}$, 15078-28-1; imidazole, 288-32-4; cyanide, 57-12-5; dimethyl sulfoxide, 67-68-5.

Contribution from the School of Chemistry,
Georgia Institute of Technology, Atlanta, Georgia 30332

Oxidative Electrochemistry of Iron–Selenocarbonyl Porphyrins

JEAN-NOEL GORCE and LAWRENCE A. BOTTOMLEY*

Received November 2, 1984

The oxidation of selenocarbonyl(5,10,15,20-tetraphenylporphinato)iron(II), (TPP)FeCSe, was studied in 1,2-dichloroethane solution at a Pt-button electrode. Results from detailed voltammetric and spectroelectrochemical experiments (both electronic and infrared) indicated that (TPP)FeCSe can be oxidized in two chemically reversible, one-electron transfers. This is comparable to thiocarbonyl iron porphyrin but is in marked contrast with the analogous carbonyl iron(II) porphyrin derivative. The latter complex loses CO concomitantly with the removal of the first electron. The product of the first oxidation of (TPP)FeCSe is a selenocarbonyl iron(III) porphyrin whereas the second oxidation step occurs at the periphery of the porphyrin ring, producing the selenocarbonyl iron(III) porphyrin cation radical. Addition of nitrogenous bases to solution generated the monoadduct, (TPP)FeCSe[nitrogenous base]. This adduct was also oxidized in two discrete, one-electron transfers. The product of the first oxidation, $\{(TPP)Fe^{III}CSe[\text{nitrogenous base}]\}^+$, was stable for hours. The product of the second oxidation, however, readily underwent nucleophilic attack by uncomplexed nitrogenous base present in solution. The electronic effects generated by the ligand trans to the selenocarbonyl moiety are discussed in the context of their influence on the spectral, electrochemical, and thermodynamic properties of the selenocarbonyliron porphyrin.

Introduction

The interaction of neutral diatomic molecules (O_2, CO, NO, CS, CSe) with synthetic iron porphyrins is being intensively investigated.[1,2] Until recently little attention has been directed toward the electrooxidation of porphyrin Fe^{II} diatomic molecule complexes. This was due, in part, to the observation of only ferrous porphyrin complexes in vivo and, in part, to unsuccessful attempts to chemically generate oxidized forms of these complexes in the laboratory. Brown et al.,[3] Gurira and Jordan,[4] and Buchler et al.[5] have attempted to electrochemically generate $[(Por)FeCO]^+$ (Por = porphyrin) complexes. In each case, oxidation of CO-bound iron(II) porphyrins proceeded with loss of CO. Similarly, oxidation of $(Por)Fe^{II}O_2$ complexes initiates a chemical reaction pathway that eventually leads to formation of either the μ-oxo dimer or the ferric monomer, depending upon conditions.[6]

Recently, both Buchler[7] and Kadish[8] have independently observed the reversible electrooxidation of $(Por)Fe^{II}NO$ complexes. The formal valence of Fe in the oxidized nitrosyl species has yet to be determined.[8b] Electrooxidation of six-coordinate $(Por)Fe^{II}NO[L]$ (L = nitrogenous base) complexes occurs irreversibly, producing the $[(Por)Fe^{II}[L]_2]^+$ species.

The reversible electrooxidations of $(Por)Fe^{II}CS$ complexes have been well documented.[5,9,10] Bottomley and co-workers[10] have demonstrated that both $(TPP)Fe^{II}CS$ and $(TPP)Fe^{II}CS[L]$ undergo two chemically reversible one-electron-transfer reactions. The electrode product resulting from the first oxidation step was found to be an extremely stable cationic ferric porphyrin. The product of the second oxidation was an Fe^{III} radical cation, whose lifetime in solution decreased in the presence of nitrogenous bases. Both electron-transfer reactions proceeded with full retention of the diatomic ligand. Gorce[11] has reported voltammetric results that indicated that the electrooxidation of $(TPP)Fe^{II}CSe$ probably proceeds by a pathway similar to that of $(TPP)Fe^{II}CS$. The uniqueness of the $Fe^{II}CSe$ moiety and the possibility of observing an $Fe^{III}CSe$ species prompted this study.

Experimental Section

Caution! The chemicals used were or were presumed to be highly toxic. Selenium-containing compounds gave off an extremely obnoxious odor. All reactions were carried out in a well-ventilated hood. Selenium-containing waste products were disposed of after treatment with sodium hypochlorite solution.

Materials. Benzylselenocyanate ($C_6H_5CH_2SeCN$) was obtained via modification of the procedure put forth by Jackson.[12] A melting point of 72–73 °C was obtained (lit.[12] mp 71.5 °C). This product was obtained in a 74% yield based on potassium selenocyanate. ^1H NMR in $CDCl_3$ referenced to $(CH_3)_4Si$ (ppm): 7.40 (s, 5 H), 4.33 (s, 2 H).

Benzyl trichloromethyl selenoether, ($C_6H_5CH_2SeCCl_3$) was obtained by following the general procedure presented by Makosza and Fedorynski[13] for their synthesis of the analogous sulfur compound. ^1H NMR

(1) Hashimoto, T.; Basolo, F. *Comments Inorg. Chem.* **1981**, *1*, 199.
(2) Jameson, G. B.; Ibers, J. A. *Comments Inorg. Chem.* **1983**, *2*, 97.
(3) Brown, G. M.; Hopf, F. R.; Meyer, T. J.; Whitten, D. G. *J. Am. Chem. Soc.* **1975**, *97*, 5385.
(4) Gurira, R. C.; Jordan, J. *Anal. Chem.* **1981**, *53*, 864.
(5) Buchler, J. K.; Kobisch, W.; Smith, P. D.; Tonn, B. *Z. Naturforsch., B: Anorg. Chem., Org. Chem.* **1978**, *33B*, 1371.
(6) Dolphin, D.; James, B. R.; Welborn, H. C. In "Electrochemical and Spectrochemical Studies of Biological Redox Components"; Kadish, K. M., Ed.; American Chemical Society: Washington, DC, 1982; Chapter 23.
(7) Buchler, J. W.; Lay, K. L. *Z. Naturforsch., B: Anorg. Chem., Org.* Chem. **1975**, *30*, 385.
(8) (a) Olson, L. W.; Schaeper, D.; Lancon, D.; Kadish, K. M. *J. Am. Chem. Soc.* **1982**, *104*, 3042. (b) Lancon, D.; Kadish, K. M. *J. Am. Chem. Soc.* **1983**, *105*, 5610. (c) Kadish, K. M.; Lancon, D.; Cocolios, P.; Guilard, R. *Inorg. Chem.* **1984**, *23*, 2372.
(9) (a) Lexa, D.; Saveant, J.-M.; Battioni, J.-P.; Lange, M.; Mansuy, D. *Angew. Chem., Int. Ed. Engl.* **1981**, *20*, 578. (b) Battioni, J.-P.; Lexa, D.; Mansuy, D.; Saveant, J.-M. *J. Am. Chem. Soc.* **1983**, *105*, 207.
(10) Bottomley, L. A.; Deakin, M. R.; Gorce, J.-N. *Inorg. Chem.* **1984**, *23*, 3563.
(11) Gorce, J.-N. *J. Electrochem. Soc.* **1984**, *131*, 35C.
(12) Jackson, C. L. *Ann. Chem.* **1875**, *179*, 1.
(13) Makosza, M.; Fedorynski, M. *Synthesis* **1974**, *274*.

0020-1669/85/1324-1431$01.50/0

in $CDCl_3$ referenced to $(CH_3)_4Si$ (ppm): 7.39 (s, 5 H), 4.60 (s, 2 H). Based on benzyl selenocyanate, the yield of benzyl trichloromethyl selenoether was 69%.

(TPP)FeCSe was synthesized following the procedure previously published for the synthesis of (TPP)FeCS except that benzyl trichloromethyl selenoether was used in place of thiophosgene.[10] The crude material can be purified by chromatography on either unactivated neutral alumina or on silica gel. The material purified by either method gave infrared ($\nu_{C=Se}$ = 1145 cm^{-1}) and electronic spectra identical with that previously published for this compound.[14] ^1H NMR in $CDCl_3$ referenced to $(CH_3)_4Si$ (ppm): 8.84 (s, 8 H), 8.14 (m, 8 H), 7.73 (m, 12 H).

All nitrogenous bases except pyridine and imidazole were purchased and used as received from the Aldrich Chemical Co. Pyridine was kept over KOH pellets and distilled from CaO in a nitrogen atmosphere just prior to use. Imidazole was recrystallized from benzene and vacuum dried for 4 h. The supporting electrolyte, tetrabutylammonium perchlorate, TBAP, was obtained from the Eastman Chemical Co. TBAP was initially vacuum dried at 110 °C for 6 h to remove bulk traces of water. Prior to use, it was recrystallized three times from absolute ethanol, vacuum dried for 24 h at 110 °C, and stored in the dark in an evacuated desiccator. The electrochemical solvent, 1,2-dichloroethane, was extracted with concentrated sulfuric acid and then with distilled, deionized water. The resultant extract was dried with anhydrous magnesium sulfate, filtered, and fractionally distilled from phosphorus pentoxide in a nitrogen atmosphere. This solvent was stored in the dark over activated 4-Å molecular sieves.

Instrumentation. Visible spectral measurements were obtained with a Tracor Northern optical multichannel analysis system. The system was composed of a Tracor Northern 6050 spectrometer containing a crossed Czerny-Turner spectrometer in association with the Tracor Northern 1710 multichannel analyzer. The source of irradiation was a xenon lamp. The spatial dispersion of the transmitted radiation was accomplished using a 300 groove/mm ruled grating. The detection device was a 512-diode array detector providing a spectral range of 305 nm in the first order. The LSI-11 minicomputer could be used to process the spectral data and store the complete absorbance spectral band in memory or could directly output the raw data to a dual Data Systems Design floppy-disk storage device for future data processing. Wavelength calibration was achieved with a holmium oxide filter. One complete spectrum could be obtained every 5.15 ms. All spectral measurements reported herein represent the ensemble averaging of at least 128 spectral acquisitions. For display purposes, a 5-point Savitsky-Golay smoothing algorithm was applied to the spectra prior to output onto a Houston Omnigraphic 2000 X-Y recorder.

Cyclic voltammetric experiments (CV) were carried out with an IBM Instruments, Inc., Model EC225 polarographic system. A conventional three-electrode system was used with a Pt-button working electrode, a Pt-wire counter electrode, and a saturated calomel electrode, SCE, as reference. The effective area of the working electrode was electrochemically calibrated as 0.0193 ± 0.006 cm^2. Aqueous contamination of electrochemical solutions from the reference electrode was minimized by isolating the reference electrode via a frit. All electrochemical experiments were carried out in 0.1 M TBAP/1,2-dichloroethane solutions at 25.0 ± 0.5 °C. Voltammograms obtained at a scan rate of 20–500 mV/s were recorded on a Houston Omnigraphic 2000 X-Y recorder. Voltammograms recorded at scan rates faster than 500 mV/s were recorded on a type 564 storage oscilloscope equipped with two type 3472 dual-trace amplifiers. To compensate for solution resistance, positive-feedback *iR* compensation was employed.

Differential-pulse voltammetric (DPV) experiments were performed with a Model EC225 polarographic system that had been modified to allow the user to select the pulse direction independently of the potential sweep direction. For all DPV experiments, a potential scan rate of 10 mV/s was employed. The pulse interval was selected at 0.1 s while pulse amplitudes varied between 5 and 100 mV.

Coulometric and chronocoulometric experiments were carried out on an EG&G Princeton Applied Research Model 173 potentiostat/galvanostat. Coulometry was executed in a specially designed microvolume sealed cell. Large surface working and counter Pt electrodes were substituted for those used in the voltammetric experiments.

All solutions were deoxygenated by passing a stream of solvent-saturated prepurified N_2 into the solution for at least 10 min prior to recording voltammetric data. To maintain an O_2-free environment, the solution was blanketed with N_2 during all experiments. All potentials reported herein were referenced to the SCE and were not corrected for liquid-junction potentials.

Spectrophotometric titrations and spectroelectrochemical experiments were performed as previously described.[10] Infrared spectroscopy was performed on a Beckman Model 4240 IR spectrometer.

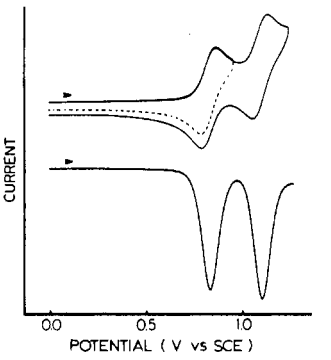

Figure 1. Voltammetric data obtained during the electrooxidation of (TPP)FeCSe in $EtCl_2$ containing 0.1 M TBAP. The upper traces are the cyclic voltammograms obtained with a potential sweep rate of 200 mV s^{-1}. The lower trace is the differential-pulse voltammogram obtained with a potential sweep rate of 10 mV s^{-1}, a pulse interval of 0.1 s, and a pulse amplitude of 25 mV.

Results

Voltammetry of (TPP)FeCSe. A preliminary study of the voltammetry of (TPP)FeCSe has been reported.[11] In the 1,2-dichloroethane solution, (TPP)FeCSe underwent two consecutive electrooxidations. Typical cyclic voltammograms depicting these events are given in Figure 1. Variable-potential scan rate studies (from 20 to 500 mV/s) were carried out on the first process. Over this range of potential sweep rates, the ratio of anodic to cathodic peak currents was equal to unity. Calculated $E_{1/2}$ values remained constant at 0.83 V. The ratio of the anodic peak current to the square root of the scan rate was found to be independent of scan rate. The separation between anodic and cathodic peak currents decreased from 96 mV at 500 mV/s to 62 mV at 20 mV/s. A separation of 59 mV would be expected for a totally reversible one-electron transfer. Furthermore, at a scan rate of 20 mV/s, $E_{p,a} - E_{p/2,a}$ and $E_{p,a} - E_{1/2}$ values were calculated to be 62 and 31 mV, respectively. Theoretical values for a totally reversible one-electron transfer are 56.5 and 28 mV, respectively.

A typical differential-pulse voltammogram of (TPP)FeCSe in solution is also shown in Figure 1. A series of differential-pulse voltammetric scans with pulse amplitudes ranging from 5 to 100 mV were carried out on the first oxidation. At a pulse amplitude of 5 mV the peak width at half-height gave a value of 104 ± 2 mV and increased to 157 ± 2 mV at a pulse amplitude of 100 mV. For a reversible one-electron transfer the peak width at half-height is expected to approach 90.4 mV as the pulse amplitude approaches zero. The potential difference between the peaks observed with positive pulses and negative pulses superimposed on the anodic potential ramp were within 1 mV of the pulse amplitude. The ratio of peak currents [$i_{p(+)}$ divided by $i_{p(-)}$] were essentially equal to 1.

Cyclic and differential-pulse voltammograms were also obtained in the characterization of the second charge-transfer event. Cyclic voltammetry results yielded an $E_{1/2}$ value of 1.11 V irregardless of potential scan rate. At a scan rate of 20 mV/s, the separation between anodic and cathodic peak was measured at 64 mV while $E_{p,a} - E_{1/2}$ gave a value of 32 mV. Both of these values increased with increasing scan rate.

Differential-pulse voltammetry on the second redox process gave results comparable to those observed for the first process. The peak currents for both processes were comparable. The peak width at half-height was measured at 102 ± 2 mV at a pulse amplitude of 5 mV. The ratio of the current peaks resulting from the positive and negative application of potential pulses on a linear ramp was again essentially unity. The potential separations between these peaks were all within 2 mV of the pulse amplitude.

(14) Battioni, J.-P.; Mansuy, D.; Chottard, J.-C. *Inorg. Chem.* **1980**, *19*, 791.
(15) Benesi, H. A.; Hildebrand, J. *J. Am. Chem. Soc.* **1949**, *71*, 2703.
(16) Bottomley, L. A.; Olson, L.; Kadish, K. M. In "Electrochemical and Spectroscopic Studies on Biological Redox Components"; Kadish, K. M., Ed.; American Chemical Society: Washington, DC, 1982; Adv. Chem. Ser. No. 201, p 279.

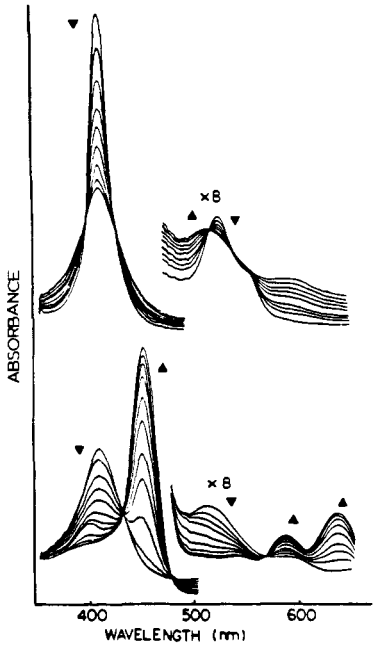

Figure 2. Time-resolved spectroelectrochemical data obtained during the electrooxidation of (TPP)FeCSe in $EtCl_2$ containing 0.1 M TBAP. The upper trace monitors the spectral interconversion upon stepping the potential from 0.27 to 0.98 V. The lower trace monitors from 0.98 to 1.26 V. Spectra were obtained every 5 s. The potential of 1.26 V was applied 90 s after the 0.98 V was applied.

Taken collectively, the voltammetric results indicated that the electrooxidation of (TPP)FeCSe in 1,2-dichloroethane was best described as two discrete, one-electron, quasi-reversible charge transfers. Chronocoulometric experiments were employed to measure the diffusion coefficient of (TPP)FeCSe ($(9.7 \pm 0.3) \times 10^{-6}$ cm^2/s). From this value and cyclic voltammetry results, the heterogeneous rate of electron transfer was computed as $(4.6 \pm 0.4) \times 10^{-2}$ cm/s. This value resided just within the boundary zone suggested by Matsuda and Ayabe[17] for a quasi-reversible electron transfer.

The chemical reversibility of the electrode oxidiations was confirmed coulometrically and spectrally. Exhaustive electrolysis at 0.97 V resulted in a charge transfer of 1.02 electrons/equiv. Subsequent electrolysis at 1.35 V resulted in a charge transfer of 1.08 electrons/equiv. Reversal of the potential to the initial potential of zero charge (0.12 V) gave a charge transfer of 2.21 electrons/equiv.

Spectroelectrochemistry of (TPP)FeCSe. To evaluate the long-term stability of the oxidation products, the electrooxidation of (TPP)FeCSe was monitored spectrally over longer time periods. A 4.21×10^{-4} M solution of the porphyrin was placed in the OTTLE. At the potential of zero current, E_{oc}, (0.293 V) the characteristic spectrum of (TPP)FeCSe was observed with an intense Soret band at 408 nm and two less predominant visible bands at 524 and 551 nm. The potential was then stepped from E_{oc} to 0.980 V and the spectral interconversion from the neutral species to be first oxidation product monitored. Spectra acquired every 5 s are shown in the upper portion of Figure 2. The interconversion was accompanied with neat isosbestic points at 395, 425, 515, and 538 nm. Coincidental with this charge transfer was a 56% loss in Soret band intensity but without wavelength shift. The α band underwent a 49-nm bathochromic shift with slight intensity gain, while the β band shifted hypsochromically by 12 nm and lost intensity. The electrode product appeared to be indefinitely stable under an applied potential. Reversal of the applied potential after 4 h regenerated the electronic spectrum characteristic of (TPP)FeCSe within 60 s.

On a fresh solution of (TPP)FeCSe, the first oxidation product was generated at an applied potential of 0.980 V. The potential was then stepped up to 1.260 V, and spectral changes were monitored as a function of time as depicted in the lower portion of Figure 2. A final spectrum was obtained within 40 s. The interconversion was accomplished with neat isosbestic points at 430, 481, and 565 nm. The Soret band shifted to 450 nm and approximately doubled in intensity. The β band almost completely disappeared while two new visible bands appeared at 581 and 636 nm. This species was stable for at least 10 min. There was a very gradual loss of Soret band intensity with time. After 60 min under an applied potential of 1.26 V, the Soret band had lost 13% of its intensity. Reversing the potential to 0.970 V and then to 0.300 V regenerated 84% of the first oxidation product and 83% of (TPP)FeCSe, respectively. When the potential was stepped back only 5 min after generation of the second oxidation product, 99% of both the first oxidation product and the neutral porphyrin were regenerated.

Multiple-potential-step chronoabsorptometry was also used to determined the temporal stability of the oxidized species. The applied potential was incrementally stepped from E_{oc} to 1.26 V, a potential where only the second oxidation product should exist. The potential step magnitude varied from 5 mV in the region where (TPP)FeCSe was electroactive to 50 mV in the region of electroinactivity. At each applied potential, a stable spectrum was always obtained within 20 s. Spectra were recorded 1 min after the application of the new potential. Spectral interconversion from the neutral species to the first oxidation product was accomplished with neat isosbestic points at 395, 425, 515, and 538 nm. In the range of 0.950–1.020 V, the observed spectrum was unchanged and was identical with that obtained by spectropotentiostatic experiment described above (Figure 2). From 1.020 to 1.260 V, spectral changes could be associated with the disappearance of the first oxidation product and the production of the second. This interconversion generated neat isosbestic points at 430, 480, and 567 nm. Upon generation of the second oxidation product from the first, the potential was held at 1.260 V for 15 min with little spectral changes. However after 15 min spectral degradation was apparent. Within 60 min the 450-nm Soret band had been reduced by 10% of its intensity. Increasing the applied potential to 1.30 V proved to quicken the spectral decay process.

Spectroscopic Characterization of (TPP)FeCSe. A solution of (TPP)FeCSe in 0.10 M TBAP/1.2-dichloroethane gave a visible spectrum with a predominent Soret band at 408 nm and a corresponding extinction coefficient of 2.24×10^{-5}. α and β bands were located at 551 nm ($\epsilon = 9 \times 10^3$) and 524 nm ($\epsilon = 17 \times 10^3$), respectively. These values are similar to those reported by Battioni and co-workers[14] for the pentacoordinated (TPP)FeCSe complex in benzene. A comparable visible spectrum was reported for the analogous (TPP)FeCS complex[5,10] except that the latter had a less intense Soret band.

Addition of nitrogenous bases to solution produced significant spectral line shifts with little or no change in the intensities of the spectral lines. Substantial red shifts were observed for all lines; the Soret band shifted from 13 to 17 nm, the α band from 17 to 24 nm, and the β band from 26 to 33 nm, depending upon the identity of the nitrogenous base added to solution. Table I lists the peak maxima and molar absorptivities observed for (TPP)-FeCSe solutions in the presence of 15 different nitrogenous bases.

To ascertain the specific interaction of the nitrogenous base with the Fe porphyrin, titration experiments were carried out and the progress of the reaction was monitored spectrophotometrically, in the manner previously described for (TPP)FeCS. Analysis of the change in absorbance at 408 and 423 nm (by the method of Benesi and Hildebrand[15]) indicated that the complexation reaction involved 1.01 ± 0.02 nitrogenous base molecules for all 15 ligands used. Duplicate titrations were carried out for each nitrogenous base.

IR spectroscopic measurements confirmed the retention of the selenocarbonyl moiety in the presence of excess nitrogenous base. In both Nujol mull and $CHCl_3$ solution, the C=Se stretch was observed at 1145 cm^{-1}. Addition of nitrogenous bases to (TPP)FeCSe (dissolved in $CHCl_3$) shifted the C=Se stretching frequency to lower energies. The specific values for the C=Se

(17) Matsuda, H.; Ayabe, T. *Z. Elektrochem.* **1955**, *59*, 494.

Table I. Spectral Data for (TPP)FeCSe[L] Complexes

ligand	elec spec features[a]			C=Se str freq,[b] cm^{-1}
none	408 (2.24)	524 (0.17)	551 (0.09)	1145
3,5-dichloropyridine	421 (2.16)	541 (0.15)	577 (0.05)	
3-cyanopyridine	421 (2.25)	542 (0.14)	578 (0.05)	1131
4-cyanopyridine	421 (1.93)	542 (0.15)	578 (0.05)	
3-chloropyridine	422 (2.19)	543 (0.15)	580 (0.05)	
3-bromopyridine	422 (2.17)	544 (0.14)	580 (0.05)	1123
3-acetylpyridine	422 (2.25)	544 (0.14)	581 (0.05)	
4-acetylpyridine	422 (2.03)	543 (0.13)	580 (0.05)	
aniline	423 (1.93)	545 (0.14)	581 (0.05)	
pyridine	423 (2.14)	544 (0.15)	582 (0.06)	1117
3-picoline	423 (2.08)	545 (0.13)	583 (0.04)	
4-picoline	423 (2.10)	545 (0.13)	582 (0.04)	
3,4-lutidine	423 (2.20)	545 (0.14)	582 (0.04)	1115
imidazole	424 (2.27)	547 (0.12)	583 (0.04)	1096
1-methylimidazole	425 (2.30)	548 (0.15)	584 (0.04)	
piperidine	425 (2.11)	544 (0.11)	580 (0.04)	

[a] Values listed are peak maxima in nm, values in parentheses are the molar absorptivities at peak maximum divided by 10^5. Solvent was 1,2-dichloroethane which was 0.1 M in TBAP. [b] Infrared measurements were made on samples prepared in Nujol.

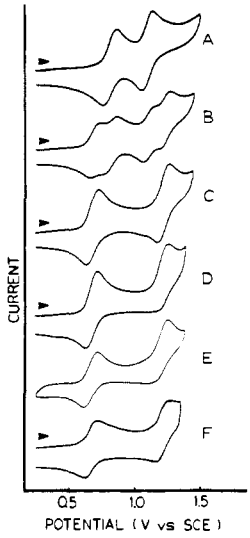

Figure 3. Cyclic voltammograms obtained during the electrooxidation of (TPP)FeCSe in $EtCl_2$ containing 0.1 M TBAP and various amounts of pyridine: (A) 0.0 equiv; (B) 0.5 equiv; (C) 1.0 equiv; (D–F) 1.2 equiv. Traces A–D were the first scan cyclic voltammograms obtained at a potential sweep rate at 100 mV s^{-1}. Trace E is the steady-state voltammogram obtained after six continuous-potential scans. Trace F is the first scan cyclic voltammogram obtained at a potential sweep rate of 3 V/s and at a current setting five times that depicted.

stretch are also listed in Table I.

Voltammetry of (TPP)FeCSe[L] Complexes. The electron-transfer properties of the (TPP)FeCSe[L] complexes were also investigated. Figure 3 shows cyclic voltammograms of (TPP)-FeCSe in solutions containing varying concentrations of pyridine. In the absence of any ligand only two oxidation processes are observed. At substoichiometric amounts of ligand (Figure 3B), four distinct electron-transfer processes are obtained. The two new processes are associated with the sequential oxidation of (TPP)FeCSe[py]. At py to porphyrin ratios greater than 1 (Figure 3C–F) the first oxidation process was found at $E_{1/2}$ = 0.70 V. Analysis of the results from variable scan rate cyclic voltammetric and chronocoulometric experiments indicated that this process can best be described as a quasi-reversible, one-electron transfer. The heterogeneous rate of electron transfer was measured at (2.5 ± 0.4) × 10^{-2} cm/s with a diffusion coefficient of (6.2 ± 0.7) × 10^{-6} cm^2/s.

In contrast, the cathodic peak current for the second electrooxidation was dependent upon the ligand concentration and the potential sweep rate (see Figure 3C–F). At a py to porphyrin ratio of 1.05, the half-wave potential of this process remained constant at 1.22 V, independent of the scan rate. The separation between the forward and reverse peak potential ranged from 85 mV at 500 mV/s to 62 mV at 20 mV/s. At 20 mV/s, the separation between the forward peak potential and the thermodynamic half-reaction potential ($E_p - E_{1/2}$) was 31 mV/s.

At higher ligand to porphyrin ratios (Figure 3D–F), the chemical reversibility of the second oxidation process depended upon the ligand to porphyrin ratio and the potential sweep rate. At a ligand to porphyrin ratio of 1.2 and a potential sweep rate of 100 mV/s (Figure 3D) the ratio of cathodic to anodic peak currents is much less than 1 and increased with increasing scan rate (Figure 3F). The anodic peak potential shifted +43 mV per 10-fold increase in scan rate. These results indicated that the second oxidation process is best described as a quasi-reversible electron transfer coupled with a chemical reaction following the charge transfer. Also, a cyclic voltammogram taken at steady state (Figure 3E) indicated that the product of the chemical reaction can be electroreduced at $E_{p,c}$ = 1.18 V, generating the starting material (TPP)FeCSe[py]. Similar results were obtained for all of the nitrogenous bases investigated. Comparison of the cyclic voltammograms obtained in the presence of excess ligand indicated that the rate of the chemical reaction following the second charge-transfer step increased with increasing basicity of the ligand.

To ascertain the specific interaction of the nitrogenous base with the oxidized forms of the iron porphyrin, differential-pulse voltammetric experiments were carried out during the titration of (TPP)FeCSe with bases listed in Table II. Figure 4 depicts the voltammograms obtained during the titration with pyridine. In the absence of pyridine, two peaks were observed at E_p = 0.84 and 1.12 V. The addition of pyridine resulted in two new processes at E_p = 0.70 and 1.24 V. Over the pyridine concentration range of 0–1 equiv, incremental additions of ligand resulted in a linear

Table II. Potential Data[a] for Oxidation of (TPP)FeCSe[L] Complexes

ligand identity	pK_{BH^+}[b]	substituent const[c]	$E_{1/2}$ (1st oxidn)	$E_{1/2}$ (2nd oxidn)
none			0.83	1.11
3,5-dichloropyridine	0.67	0.74	0.79	1.21
4-cyanopyridine	1.85	0.66	0.77	1.23
3-bromopyridine	2.84	0.39	0.76	1.24
4-acetylpyridine	3.51	0.22	0.75	1.23
pyridine	5.28	0.00	0.70	1.22
3-picoline	5.77	−0.07	0.69	1.21
4-picoline	5.98	−0.17	0.69	1.22
3,4-dimethylpyridine	6.46	−0.24	0.68	1.21
imidazole	6.65		0.62	1.17

[a] Measured at 25 ± 2 °C in 0.1 M TBAP/$EtCl_2$. [b] Values taken from: Schoefield, K. S. "Hetero-Aromatic Nitrogen Compounds"; Plenum Press: New York, 1967; p 146. [c] Values taken from: Jaffe, H. H. *Chem. Rev.* **1953**, *53*, 191.

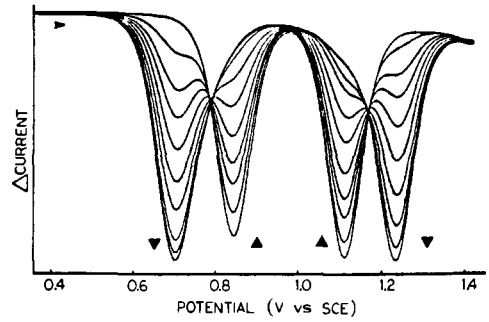

Figure 4. Differential-pulse voltammograms obtained during the titration of (TPP)FeCSe with pyridine. The scans depicted were taken over the pyridine concentration range of 0.0–1.1 equiv. The pertinent instrumental parameters were a potential sweep rate of 10 mV/s, a pulse interval of 0.1 s, and a pulse amplitude of 25 mV.

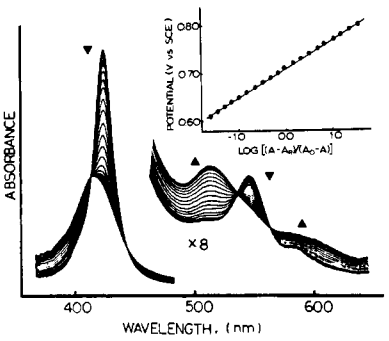

Figure 5. Spectra obtained during the incremental potential step experiment on a solution of (TPP)FeCSe containing 1.05 equiv of pyridine in $EtCl_2$ and 0.1 M TBAP over the potential range at 0.50–1.00 V. The inset depicts a Nernst plot providing analysis of the absorbance at 408 nm vs. applied potential.

decrease in the peak currents for the processes at E_p = 0.84 and 1.12 V and a linear increase in the peak currents at E_p = 0.70 and 1.24 V. At pyridine to porphyrin ratios greater than 1, only the processes at E_p = 0.70 and 1.24 V were observed. The peak current for the first charge-transfer process was independent of pyridine concentration. Analysis of the peak currents as a function of ligand concentration indicated that only one pyridine molecule was coordinating with the starting material as well as both oxidized forms.

Similar results were obtained for the other nitrogenous bases used in this study. Half-wave potentials for the sequential oxidation of the (TPP)FeCSe[L] complexes investigated are listed in Table II.

Spectroelectrochemistry of (TPP)FeCSe[L] Complexes. A multiple-potential-step chronoabsorptometric experiment was performed on a 3.82×10^{-4} M solution of (TPP)FeCSe[py]. Figure 5 depicts the spectra collected over the potential range 0.30–1.05 V. Between 0.30 and 0.60 V, the characteristic spectrum of (TPP)FeCSe[py] was observed. As the potential was incremented in 10-mV steps from 0.60 to 0.84 V, the Soret band decreased in intensity and shifted from 423 to 414 nm. The β band shifted from 545 to 516 nm and the α band shifted from 582 to 600 nm. Well-defined isosbestic points were observed at 411, 440, 534, and 560 nm. The inset of Figure 5 depicts a Nernst plot constructed from the absorbance changes observed at 408 nm. The Nernst plot confirmed that the oxidation of (TPP)-FeCSe[py] involved a one-electron transfer at a formal potential of 0.70 V. The final spectrum depicted in Figure 5 is the spectrum of the $\{(TPP)FeCSe[py]\}^+$ species. This spectrum was observed as the potential was stepped from 0.84 to 1.05 V. At any applied potential more positive than 1.05 V, no stable spectra could be obtained. This indicated the presence of a chemical reaction coupled to the second charge transfer.

To evaluate the temporal stability of the oxidized adducts, a single-step chronoabsorptometric experiment was performed. When the potential was stepped from the potential of zero current to 0.93 V on a fresh solution of (TPP)FeCSe[py], a stable spectrum was observed within 70 s. The spectrum was identical with the final spectrum depicted in Figure 5. The interconversion generated the same isosbestic points as previously observed in the multiple-step experiment. Under an applied potential of 0.93 V, $\{(TPP)FeCSe[py]\}^+$ was stable for at least 3 h. Stepping the potential back to 0.30 V quantitatively regenerated (TPP)FeC-Se[py].

When the potential was stepped from 0.93 to 1.35 V, the Soret band at 415 nm decreased in intensity and a new band appeared at 445 nm. An isosbestic point was observed 430 nm only during the first 30 s of the electrolysis. The new Soret band reached maximum intensity at 60 s. During this time, both the α and β bands lost intensity, with the β band shifting to 570 nm. After 60 s, the Soret band rapidly lost intensity, shifting to 455 nm, and the visible bands disappeared. When the potential was maintained at 1.35 V for 120 s and then stepped back to 0.93 V, 67% of the first oxidation product was regenerated. When the potential was stepped back to 0.30 V, 75% of the starting species (TPP)FeC-Se[py] was regenerated in the OTTLE.

Scheme I

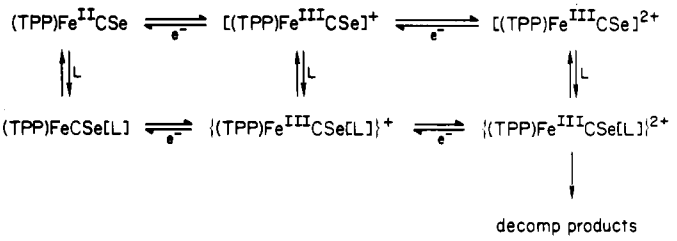

Discussion

Electrode Mechanism for Oxidation of (TPP)FeCSe. Taken collectively, the voltammetric results indicated that the electrooxidation of (TPP)FeCSe proceeded in two discrete, single-electron, quasi-reversible steps, as shown in the upper portion of Scheme I. The product of the first electron transfer is assigned as a selenocarbonyliron(III) porphyrin for the following reasons: First, the spectral interconversion between the starting material and the first oxidation product was chemically reversible and characterized by well-defined isosbestic points. The electronic spectrum of the product possessed features characteristic of iron(III) porphyrins, i.e. diminished Soret band intensity (as compared to the Fe(II) starting material) and an increase in separation between the α and β bands.[18] Second, the IR stretch characteristic of (TPP)Fe cation radicals[19] was not present in the spectrum taken on oxidized material. Third, the voltammetric and spectroelectrochemical results were analogous to those observed for (TPP)FeCS.[10] Last, the IR vibration previously assigned to the C–Se stretch (at 1145 cm^{-1}) shifted to 1240 cm^{-1} upon oxidation. To our knowledge, this is the first example of a selenocarbonyliron(III) complex. However, the spectral shift is consistent with expectations for coordination of the C=Se moiety to a more electropositive metal center.

The product of the second oxidation step is formally assigned as a selenocarbonyliron(III) porphyrin cation radical. This assignment is based on the following observations: First, the electronic spectrum is comparable to that previously observed for porphyrin cation radicals.[20] Second, the chemical reversibility of the second oxidation reaction during the spectroelectrochemical experiments as well as the absence of the chemistry expected for free :C=Se strongly infers retention of the selenocarbonyl moiety on the Fe(III) porphyrin cation radical. Third, the voltammetric and spectroelectrochemical results are completely analogous to those observed for (TPP)FeCS in which the diatomic ligand remains coordinated to the Fe center.

Electrode Mechanism for Oxidation of (TPP)FeCSe[L] Complexes. The electron-transfer pathway for electrooxidation of (TPP)FeCSe[L] is shown in the lower portion of Scheme I. The first oxidation of (TPP)FeCSe[L] yields a six-coordinate, unsymmetrically substituted selenocarbonyliron(III) porphyrin. The second oxidation occurs at the porphyrin ring, yielding a six-coordinate Fe(III) porphyrin cation radical. The radical is rapidly decomposed via nucleophilic attack by excess nitrogenous base present in solution. The rationale behind these assignments follows the lines presented above.

It is now well established that the half-wave potential can be an indicator of the ultimate site of electron transfer.[10,16,21,22] The

(18) (a) Felton, R. H. In "The Porphyrins"; Dolphin, D., Ed.; Academic Press: New York, 1979; Vol. V, Chapter 3. (b) Walker, F. A.; Lo, M.-W.; Ree, M. T. *J. Am. Chem. Soc.* **1976**, *98*, 5552.
(19) Shimomura, E. T.; Phillippi, M. A.; Goff, H. M.; Scholz, W. F.; Reed, C. A. *J. Am. Chem. Soc.* **1981**, *103*, 6778.
(20) (a) Carnieri, N.; Harrison, A. *Inorg. Chim. Acta* **182**, *62*, 103. (b) Wollberg, A.; Manassen, J. *J. Am. Chem. Soc.* **1970**, *92*, 1982. (c) Gans, P.; Marchon, J. C.; Regnard, J. R. *Nouv. J. Chim.* **1981**, *5*, 203.
(21) (a) Bottomley, L. A.; Kadish, K. M. *Inorg. Chem.* **1981**, *20*, 1348. (b) Kadish, K. M.; Bottomley, L. A. *Ibid.* **1980**, *19*, 832.

Table III. Formation Constants[a] for (TPP)FeCSe[L] Adducts

ligand identity	pK_{BH^+}[b]	substituent const[d]	log B	log B^{+}[c]	log B^{2+}[e]
3,5-dichloropyridine	0.67	0.74	2.64 ± 0.09	3.3	1.6
3-cyanopyridine	1.45	0.68	2.80 ± 0.08		
4-cyanopyridine	1.85	0.66	3.10 ± 0.07	4.1	2.1
3-chloropyridine	2.81	0.37	3.23 ± 0.06		
3-bromopyridine	2.84	0.39	3.32 ± 0.13	4.5	2.3
3-acetylpyridine	3.18	0.38	3.55 ± 0.04		
4-acetylpyridine	3.51	0.22	3.53 ± 0.06	4.9	2.7
aniline	4.63		2.92 ± 0.11		
pyridine	5.28	0.00	3.74 ± 0.05	5.9	3.9
3-picoline	5.77	−0.07	3.87 ± 0.05	6.2	4.5
4-picoline	5.98	−0.17	3.90 ± 0.14	6.3	4.4
3,4-dimethylpyridine	6.46	−0.24	3.95 ± 0.10	6.5	4.8
imidazole	6.65		4.24 ± 0.13	7.8	6.8
1-methylimidazole	7.33		4.63 ± 0.14		
piperidine	11.10		5.02 ± 0.07		

[a] Measured at 25 ± 2 °C in 0.1 M TBAP/$EtCl_2$. [b] Values taken from: Schoefield, K. S. "Hetero-Atomatic Nitrogen Compounds"; Plenum Press: New York, 1967; p 146. [c] Uncertainties are ±0.2 in the log unit. [d] Values taken from: Jaffe, H. H. *Chem. Rev.* **1953**, *53*, 191. [e] Uncertainties are ±0.3 in the log unit.

potential for oxidation of the porphyrin ring is independent of the basicity of the Fe center's axial ligand. Inspection of the potential data reported for both oxidations (Table II) revealed that the first oxidation is linearly related to the basicity of the nitrogenous base whereas the second oxidation process is independent of the axial ligand's basicity. This provided confirming evidence for the assignments of the ultimate site of electron transfer in the selenocarbonyliron porphyrin system.

Formation Constants for Ligand Addition. On the basis of absorbance changes as a function ligand concentration, formation constants (as defined in eq 1) for addition of one nitrogenous base

$$B^0 = [(TPP)Fe^{II}CSe[L]]/[(TPP)Fe^{II}CSe][L] \quad (1)$$

(TPP)FeCSe were computed. The values obtained for the nitrogenous bases utilized are listed in Table III. Formation constants (as defined in eq 2 and 3) for addition of one nitrogenous

$$B^{+} = [\{(TPP)Fe^{III}CSe[L]\}^{+}]/[\{(TPP)Fe^{III}CSe\}^{+}][L] \quad (2)$$

$$B^{2+} = [\{(TPP)Fe^{III}CSe[L]\}^{2+}]/[\{(TPP)Fe^{III}CSe\}^{2+}][L] \quad (3)$$

base to the Fe(III) and the Fe(III) porphyrin cation radical were computed from the half-wave potential data in the usual fashion[16] and are also listed in Table III.

The magnitudes of the formation constants for ligand addition were found to be linearly related to the pK_{BH^+} of the substituted pyridine ligand. Linear least-squares analysis of log B^0, log B^{+}, and log B^{2+} vs. pK_{BH^+} gave slopes of 0.21, 0.53, and 0.58, respectively. These values compare favorably with those previously reported for ligand addition to (TPP)FeCS and indicate that the ligand-to-metal interaction is predominately σ. Linear relationships were also obtained when the log of the formation constant was plotted vs. the Hammett–Taft substituent constant for each substituted pyridine.

Comparison of (TPP)FeCX (Where X = O, S, and Se) Reactivity. It is interesting to compare the redox behavior of the three Fe porphyrin complexes possessing isoelectronic diatomic axial ligands. The observation of two, chemically reversible oxidations for the selenocarbonyliron(II) porphyrin mirrors that observed for the thiocarbonyl complex and contrasts with the reactivity of the analogous CO complexes. In all cases reported to date, oxidation of the carbon monoxide bound iron(II) porphyrin proceeds with concomitant loss of the CO. The oxidation of CS- and CSe-bound iron porphyrins is energetically more difficult than the corresponding CO complexes and produces novel $Fe^{III}CS$ and $Fe^{III}CSe$ moieties. These observations are consistent with CS and CSe being better σ-donor and π-acceptor ligands than CO.[23] The $E_{1/2}$ values for the first and second oxidations of (TPP)FeCS[10] are 0.85 and 1.16, respectively, whereas the corresponding values for the selenocarbonyl complex are 0.83 and 1.11 V. Thus, the Fe^{II}/Fe^{III} redox couple is 20 mV and the Fe^{III}/cation radical step is 50 mV less positive for the CSe adduct as compared to the CS adduct. Similarly, the $E_{1/2}$ values for the stepwise oxidation of (TPP)FeCSe[L] complexes were, on the average, 30 and 70 mV lower than the corresponding FeCS[L] adduct. Although it may be tempting to rationalize this trend on the basis of CS being a slightly stronger π acceptor than CSe, no explanation can be given until the Fe^{III} complexes have been fully characterized.

We[10] and others[24] have shown that the C=S stretching frequency for (TPP)FeCS[L] complexes is dependent upon the identity of L. The frequency shifts to lower wavenumbers as the basicity of the ligand trans to the C=S moiety increases. Similar results were observed for (TPP)FeCSe[L] complexes. For example, the $\nu_{C=S}$ observed for the five-coordinate (TPP)FeCS complex was 1308 cm^{-1}. Addition of one pyridine molecule trans to CS shifted $\nu_{C=S}$ to 1295 cm^{-1}. The five-coordinate selenocarbonyl complex gave a $\nu_{C=Se}$ at 1145 cm^{-1}. Addition of one pyridine molecule trans to CSe shifted $\nu_{C=Se}$ to 1117 cm^{-1}. Oxidation of the (TPP)FeCS complex resulted in a shifting of $\nu_{C=S}$ from 1308 to 1374 cm^{-1} whereas the selenocarbonyl complex shifted from 1145 to 1240 cm^{-1}. Whether these shifts result from differences in the σ-donor and/or π-acceptor ability of CS vs. CSe awaits careful analysis of the Fe–C vibrational modes. Such studies are now under way.

Acknowledgment is made by J.-N.G. to the Electrochemical Society, Inc., for an Energy Research Summer Fellowship sponsored by the Department of Energy. Acknowledgment is also made to the donors of the Petroleum Research Fund, administered by the American Chemical Society, and the Cottrell Grants Program of the Research Corp. for the support of this research. We thank Professor K. Barefield for many helpful discussions.

(22) (a) Phillippi, M. A.; Shimomura, E. T.; Goff, H. M. *Inorg. Chem.* **1981**, *20*, 1322. (b) Phillippi, M. A.; Goff, H. M. *J. Am. Chem. Soc.* **1982**, *104*, 6026.

(23) (a) Butler, I. S. *Acc. Chem. Res.* **1977**, *10*, 359. (b) Butler, I. S.; Fenster, A. E. *J. Organomet. Chem.* **1974**, *66*, 161.

(24) (a) Battioni, J.-P.; Chottard, J.-C.; Mansuy, D. *J. Am. Chem. Soc.* **1978**, *100*, 4311. (b) Battioni, J.-P.; Chottard, J.-C.; Mansuy, D. *Inorg. Chem.* **1982**, *21*, 2056.